

## The Thermal Conductivity of 1-Chloro-1,1-Difluoroethane (HCFC-142b)

A. T. Sousa,<sup>1</sup> P. S. Fialho,<sup>1</sup> C. A. Nieto de Castro,<sup>1</sup> R. Tufeu,<sup>2</sup> and  
B. Le Neindre<sup>2</sup>

*Received August 9, 1991*

---

The thermal conductivity of 1-chloro-1,1-difluoroethane (HCFC-142b) has been measured in the temperature range 290 to 504 K and pressures up to 20 MPa with a concentric-cylinder apparatus operating in a steady-state mode. These temperature and pressure ranges cover all fluid states. The estimated accuracy of the method is about 2%. The density dependence of the thermal conductivity has been studied in the liquid region.

---

**KEY WORDS:** concentric cylinder apparatus; 1-chloro-1,1-difluoroethane; thermal conductivity.

### 1. INTRODUCTION

Since the negotiation of the Montreal protocol in 1987 to limit the production of certain chlorofluorocarbons, also called CFCs or halocarbons, there has been a change in attention devoted to the study of the thermophysical properties of these fluids. The search for environmentally safe refrigerants, with a low ozone depletion potential and low contribution to the global earth warming, has increased, and define criteria that a fluid should satisfy as a safe refrigerant or foam blowing agent have been established [1, 2]. The alternative compounds are ethane derivatives, with more fluor and less chlorine, and they always have hydrogen atoms.

Among these alternative hydrochlorofluorocarbons (HCFCs) 1-chloro-1,1-difluoroethane (HCFC-142b) has a low ozone depletion potential<sup>3</sup>

---

<sup>1</sup> Departamento de Química, Faculdade de Ciências, Universidade de Lisboa, Campo Grande, Bloco C1, 1700 Lisboa, Portugal.

<sup>2</sup> LIMPH-CNRS, Université Paris Nord, 93430 Villetaneuse, France.

<sup>3</sup> Relative to CFC11 on a per-pound basis.

(0.06) and a low global warming potential<sup>3</sup> (0.41). It is slightly inflammable, has a low toxicity, and is chemically inert to most usual metals, plastic materials, and elastomers used in industry. It is already in commercial production and it is used in aerosol propellers of perfumes and shaving foams, as a plastic foam blowing agent (polyethylene and polystyrene foams), in air-conditioning, and in heat pumps that work at high temperatures as a replacement for CFC-114.

The lack of experimental thermophysical property data of good quality for this fluid justified our effort to measure the thermal conductivity of HCFC-142b as a function of temperature and pressure, from the gas to the liquid state, including the supercritical region.

Measurements of the thermal conductivity of this fluid are scarce and are restricted to the dilute gas phase [3, 4] and the low-pressure liquid [5] close to the saturation line. A set of tables was found in the literature [6]. All these data have a limited accuracy, with errors of 3% or higher. In this paper, an extensive study of the thermal conductivity of 1-chloro-1,1-difluoroethane, covering the subcritical region (290, 293, 330, 368, and 403 K), and the supercritical region (415, 426, 444, and 504 K), from 0.4 to 20 MPa, is reported.

## 2. EXPERIMENTAL PROCEDURE

The method used to measure the thermal conductivity of 1-chloro-1,1-difluoroethane was the vertical coaxial cylinder method, operating in the steady-state mode and described in detail in previous publications [7–9].

The primary measurements in this method are the voltage difference and the current intensity in the heating element, located inside the inner cylinder, along its axis, and the temperature difference between the outside wall of the inner cylinder and the inner wall of the outer cylinder. The first set of measurements permits the evaluation of the amount of heat evolved from the inner cylinder, while the second measurement is achieved by using eight Pt/Pt-Rh 10% thermocouples in series, four in each cylinder. Temperature differences  $\Delta T$  of about 2 K were used outside the critical region; in the critical region temperature differences of 0.2 to 0.8 K were used. The precision of the temperature difference measured was 0.003 K and the cell temperature was measured with a thermocouple located in the external cylinder, with an accuracy of 0.1 K.

The cell is located in a high-pressure vessel heated externally by coils wound on a copper block. High pressures were obtained by a bellow system using nitrogen from a normal gas cylinder. The pressure was measured with a Bourdon gauge calibrated to within 2 kPa with a deadweight gauge. The readings were accurate to 5 kPa.

The thermal conductivity was obtained from [10, 11]

$$\lambda_{\text{cond}} = (\lambda_m - \lambda_p)/(1 + \alpha) \quad (1)$$

where

$$\lambda_m = WK/\Delta T \quad (2)$$

is the uncorrected value of the thermal conductivity obtained from the directly measured variables,  $W = VI$  is the amount of heat emitted from the inner cylinder, and  $\Delta T$  is the temperature difference between the two cylinders. The term  $K$  is the geometrical constant of the cell, calibrated using capacitance measurements [7]. The term  $\lambda_p$  accounts for heat losses by conduction through the cylinder element, electric leads, and ceramic supports and has been previously defined as a function of  $\lambda_m$  [7-9]. The factor  $\alpha$  is the ratio between the radiative and the conductive fluxes,  $Q_{\text{rad}}$  and  $Q_{\text{cond}}$ , and it is given by

$$\alpha = \frac{Q_{\text{rad}}}{Q_{\text{cond}}} = \frac{\lambda_{\text{rad}}}{\lambda_{\text{cond}}} \simeq \frac{4S\sigma\epsilon T_1^3 \Delta T}{VI} \quad (3)$$

where  $\lambda_{\text{rad}}$  is the radiative component of the thermal conductivity,  $S$  the surface of the emitter ( $S = 8 \times 10^{-3} \text{ m}^2$ ),  $\epsilon$  the emissivity of silver, the cell material ( $\epsilon = 0.02$ ),  $\sigma$  the Stefan-Boltzmann constant, and  $T_1$  the temperature of the fluid. Although Eq. (3) assumes that the fluid is not a participant in the heat transfer by radiation, it is the best approximation for this quantity in gases and liquids at low temperatures. The lack of a complete treatment of heat transfer by radiation in concentric-cylinder instruments degrades the accuracy of the experimental measurements obtained, which is estimated to be 2%. The factor  $\alpha$  was always smaller than  $2.7 \times 10^{-3}$  in the present measurements.

Measurements were made along isotherms at decreasing pressures. As it is very difficult to maintain the temperature of the cell during a pressure scan, especially in the low-density zone where cell equilibration takes longer, the values of the thermal conductivity were corrected to a nominal temperature by

$$\lambda(\rho, T_{\text{nom}}) = \lambda(\rho, T) + (\partial\lambda/\partial T)_{\rho, T_{\text{nom}}} (T_{\text{nom}} - T) \quad (4)$$

The value of  $(\partial\lambda/\partial T)_{\rho, T_{\text{nom}}}$  was assumed to be equal to  $(d\lambda/dT)_{0, T}$ ,<sup>4</sup> evaluated from Eq. (6), as in previous works.

<sup>4</sup>This replacement is valid if the excess thermal conductivity, defined by Eq. (8), is only density dependent, which is demonstrated for this fluid in Section 4.2.

These corrections did not exceed 0.5% and, therefore, do not introduce any additional uncertainty in the data. The values of the thermal conductivity in the supercritical region were corrected only to nominal temperatures far from the critical region, because the critical enhancement is known to be strongly density and temperature dependent [10, 11].

The 1-chloro-1,1-difluoroethane was supplied by ATOCHEM, with a purity greater than 0.85%.

### 3. RESULTS

The results for the liquid and gas region are presented in Table I, for the nominal temperatures 290, 293, 330, 368, and 403 K. Table I includes the thermal conductivity at different temperatures and pressures and the values corrected to nominal temperatures. The tables also display the density of 1-chloro-1,1-difluoroethane obtained by us using a mechanical oscillator densimeter and published elsewhere [12]. The values of the density obtained in that work, together with the saturation line values of Maezawa et al. [13], were fitted to the equation of state of hard spheres, correct to the tenth virial coefficient,

$$\frac{PV}{RT} = \sum_{i=1}^{10} C_i \left(\frac{b}{V}\right)^{i-1} - \frac{a}{RT(V+b)} \quad (5)$$

compensated for long-range attractive forces by a semiempirical term, previously suggested by DeSantis et al. [14]. The hard-sphere fluid values were taken from the works of Ree and Hoover [15] and Erpenbeck and Wood [16]. The coefficients  $a$  and  $b$  were found to be temperature dependent as quadratics,

$$a = a_0 + a_1 T + a_2 T^2 \quad (6)$$

$$b = b_0 + b_1 T + b_2 T^2 \quad (7)$$

with  $a$  expressed in  $\text{J} \cdot \text{m}^3 \cdot \text{mol}^{-2}$  and  $b$  in  $\text{m}^3 \cdot \text{mol}^{-1}$ . Table II gives the values of the coefficients  $a_i$  and  $b_i$  in Eqs. (5), (6), and (7), and the hard-sphere virial coefficients were taken from Refs. 15 and 16.

Figure 1 displays the deviations of the experimental densities from those obtained by Eq. (5). It can be seen that the deviations are never greater than  $\pm 0.8\%$  in the liquid phase, except for the 403 K isotherm at high pressures and the saturation values above this temperature. Not enough experimental points exist in this region to improve the fit. This is commensurate with the uncertainties of the experimental data of

Table I. The Thermal Conductivity of HCFC-142b

$T$ (K)	$P$ (MPa)	$\rho$ ( $\text{kg} \cdot \text{m}^{-3}$ )	$\lambda(T, \rho)$ ( $\text{mW} \cdot \text{m}^{-1} \cdot \text{K}^{-1}$ )	$\lambda(T_{\text{nom}}, \rho)$ ( $\text{mW} \cdot \text{m}^{-1} \cdot \text{K}^{-1}$ )
$T_{\text{nom}} = 290 \text{ K}$				
289.7	16.56	1176	91.58	91.60
290.0	13.25	1167	89.93	89.93
290.7	10.24	1158	88.15	88.10
290.8	7.12	1150	86.36	86.30
291.0	4.52	1143	84.89	84.82
291.2	2.48	1136	83.70	83.62
291.2	0.49	1131	82.52	82.44
$T_{\text{nom}} = 293 \text{ K}$				
292.7	18.96	1176	91.39	91.41
293.0	16.26	1169	90.23	90.23
293.2	14.61	1164	88.93	88.92
293.5	11.69	1156	87.84	87.80
293.7	9.16	1149	86.56	86.51
293.9	6.64	1142	85.04	84.97
294.9	4.58	1134	84.02	83.88
295.3	2.53	1127	82.27	82.10
295.6	0.51	1120	81.35	81.16
$T_{\text{nom}} = 330 \text{ K}$				
328.2	17.07	1100	80.04	80.18
328.4	17.07	1099	80.00	80.12
329.2	14.71	1089	78.85	78.91
329.4	14.71	1089	78.77	78.82
330.4	12.35	1077	77.11	77.08
330.5	12.35	1077	77.14	77.10
330.7	9.73	1065	75.45	75.40
330.8	7.11	1054	73.77	73.71
331.0	5.09	1044	72.28	72.20
331.1	3.01	1034	70.73	70.64
331.1	0.99	1023	69.18	69.09
329.5	0.75		14.62	14.66
329.5	0.64		13.90	13.94
329.5	0.50		13.80	13.84
329.4	0.37		13.75	13.80

Table I. (Continued)

$T$ (K)	$P$ (MPa)	$\rho$ ( $\text{kg} \cdot \text{m}^{-3}$ )	$\lambda(T, \rho)$ ( $\text{mW} \cdot \text{m}^{-1} \cdot \text{K}^{-1}$ )	$\lambda(T_{\text{nom}}, \rho)$ ( $\text{mW} \cdot \text{m}^{-1} \cdot \text{K}^{-1}$ )
$T_{\text{nom}} = 368 \text{ K}$				
367.2	15.97	1009	70.77	70.84
367.7	13.22	990.6	68.60	68.62
368.1	10.73	972.5	66.64	66.63
368.6	8.18	951.9	64.40	64.35
368.7	6.07	934.2	62.51	62.46
368.9	4.05	915.4	60.44	60.37
369.0	2.00	894.5	58.09	58.01
367.9	1.80		18.36	18.44
368.0	1.49		17.49	17.49
367.8	1.19		17.02	17.04
367.8	0.78		16.66	16.68
367.7	0.40		16.38	16.40
$T_{\text{nom}} = 403 \text{ K}$				
402.8	14.94	913.2	62.33	62.25
403.1	12.50	885.9	59.99	59.98
403.3	10.12	855.7	57.71	57.68
403.6	8.51	831.8	56.05	56.00
403.7	7.03	807.8	54.66	54.60
403.8	5.40	777.1	52.74	52.67
403.8	3.80	741.3	50.74	50.67
402.5	3.50		29.51	29.55
402.5	2.80		22.72	22.76
402.3	2.12		20.66	20.72
402.3	1.48		19.84	19.90
402.4	0.91		19.55	19.60
402.4	0.48		19.30	19.35

Sousa et al. [12] and Maezawa et al. [13]. Details of this analysis can be found in Ref. 17.

Table III presents the values obtained in the supercritical region ( $T_c = 410.25 \text{ K}$ ,  $P_c = 4.246 \text{ MPa}$  [18]) for the nominal temperatures 415, 426, 444, and 504 K. As mentioned in the preceding section, the values of thermal conductivity were corrected only to nominal temperatures far from the critical point, e.g., for  $P < 4 \text{ MPa}$  and  $P > 4.8 \text{ MPa}$  in the isotherm for  $T = 415 \text{ K}$ . No data for the density of HCFC-142b in the supercritical region exist, so we present only the values of temperature, pressure, and thermal conductivity.

**Table II.** Values of the Coefficients in Eqs. (5), (6), and (7)<sup>a</sup>

<i>i</i>	<i>a<sub>i</sub></i>
0	16.1258655 J · m <sup>3</sup> · mol <sup>-2</sup>
1	-0.05862149 J · m <sup>3</sup> · mol <sup>-2</sup> · K <sup>-1</sup>
2	0.56860017 J · m <sup>3</sup> · mol <sup>-2</sup> · K <sup>-2</sup>

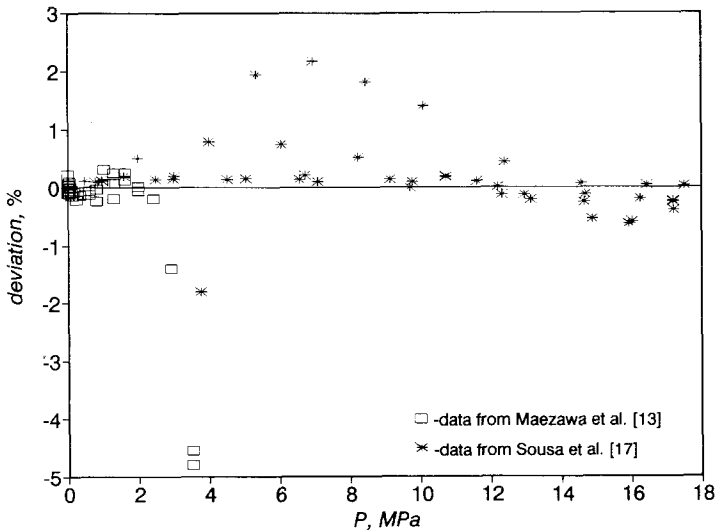
  

<i>i</i>	<i>b<sub>i</sub></i>
0	1.8268776 × 10 <sup>-4</sup> m <sup>-3</sup> · mol <sup>-1</sup>
1	6.7597368 × 10 <sup>-9</sup> m <sup>-3</sup> · mol <sup>-1</sup> · K <sup>-1</sup>
2	-4.96367419 × 10 <sup>-10</sup> m <sup>-3</sup> · mol <sup>-1</sup> · K <sup>-2</sup>

<i>i</i>	<i>C<sub>i</sub></i>
1	1
2	1
3	5/8
4	0.28695
5	0.1103 ± 0.0003
6	0.0386 ± 0.0004
7	0.0137 ± 0.006
8	0.00421
9	0.00131
10	0.00040

<sup>a</sup> The values of *C<sub>i</sub>* were taken from Refs. 15 and 16.



**Fig. 1.** Deviation of density data for 1-chloro-1,1-difluoroethane (HCFC-142b) from Eq. (5). (□) Data from Ref. 13; (\*) data from Ref. 17.

Table III. Thermal Conductivity of HCFC-142b in the Supercritical Region

$T$ (K)	$P$ (MPa)	$\lambda(T, \rho)$ (mW · m <sup>-1</sup> · K <sup>-1</sup> )	$\lambda(T_{\text{nom}}, \rho)$ (mW · m <sup>-1</sup> · K <sup>-1</sup> )
$T_{\text{nom}} = 415 \text{ K}, \Delta T = 0.8 \text{ K}$			
414.99	19.08	63.32	63.32
415.11	17.06	61.99	61.98
415.19	15.04	60.35	60.33
415.20	13.04	58.41	58.39
415.31	11.08	56.38	56.35
415.33	9.10	54.20	54.17
415.33	7.62	52.30	52.27
415.35	6.58	50.89	50.86
415.33	5.80	49.78	49.75
415.36	5.26	49.01	48.98
415.47	4.95	48.76	
415.50	4.84	48.81	
415.49	4.79	48.87	
415.51	4.75	49.04	
415.51	4.70	49.35	
415.50	4.65	50.03	
415.50	4.61	51.08	
415.46	4.56	52.81	
415.50	4.51	56.13	
415.50	4.45	57.61	
415.53	4.42	54.21	
415.55	4.40	50.22	
415.63	4.36	44.04	
415.73	4.31	40.01	
415.76	4.25	36.74	
415.80	4.20	34.77	
415.81	4.14	32.99	
$T_{\text{nom}} = 415 \text{ K}, \Delta T = 0.2 \text{ K}$			
414.93	5.01	48.30	
414.95	4.77	48.45	
414.95	4.63	49.19	
414.98	4.58	49.95	
414.96	4.54	50.81	
414.96	4.50	52.35	
414.96	4.47	54.77	
414.95	4.45	56.79	
414.95	4.42	59.14	
414.93	4.40	59.55	
414.93	4.39	58.38	
414.95	4.37	54.91	
414.97	4.36	52.59	
414.99	4.34	49.13	



Table III. (Continued)

$T$ (K)	$P$ (MPa)	$\lambda(T, \rho)$ (mW · m <sup>-1</sup> · K <sup>-1</sup> )	$\lambda(T_{\text{nom}}, \rho)$ (mW · m <sup>-1</sup> · K <sup>-1</sup> )
$T_{\text{nom}} = 415 \text{ K}, \Delta T = 0.2 \text{ K}$			
414.96	4.32	45.31	
414.97	4.29	42.45	
414.95	4.26	39.35	
414.95	4.19	36.13	
414.91	4.13	33.15	
414.77	4.04	31.98	
414.95	3.84	28.38	28.38
414.97	3.56	25.88	25.88
414.99	3.24	24.35	24.35
415.02	2.85	23.00	23.00
415.01	2.47	22.23	22.23
415.04	2.03	21.48	21.48
415.01	1.61	21.34	21.34
414.99	1.19	21.05	21.05
414.99	0.79	20.65	20.65
414.93	0.39	20.15	20.16
$T_{\text{nom}} = 426 \text{ K}$			
425.52	20.38	62.86	62.90
425.76	18.27	61.24	61.26
425.84	16.24	59.51	59.52
426.00	14.21	57.67	57.67
426.18	12.17	55.59	55.57
426.23	10.18	53.63	53.61
426.26	8.64	51.75	51.73
426.31	7.09	49.53	49.50
426.38	6.09	47.77	47.74
426.40	5.55	47.11	47.07
426.38	5.25	45.41	
426.46	5.06	42.50	
426.47	4.93	39.01	
426.57	4.78	36.29	
425.03	4.65	34.80	
425.10	4.42	31.54	
425.17	4.20	29.34	
425.33	4.02	27.77	27.83
425.33	3.65	25.71	25.77
425.31	3.22	24.36	24.42
425.29	2.81	23.44	23.50
425.31	2.40	22.76	22.82
425.42	1.72	22.53	22.58
425.51	0.80	21.71	21.75
425.55	0.49	21.24	21.28

Table III. (Continued)

$T$ (K)	$P$ (MPa)	$\lambda(T, \rho)$ (mW · m <sup>-1</sup> · K <sup>-1</sup> )	$\lambda(T_{\text{nom}}, \rho)$ (mW · m <sup>-1</sup> · K <sup>-1</sup> )
$T_{\text{nom}} = 444 \text{ K}$			
444.43	18.16	58.11	58.07
444.53	16.25	56.58	56.53
444.58	14.37	54.53	54.48
444.67	12.32	52.36	52.30
444.68	10.54	49.99	49.93
444.60	9.13	47.88	47.83
444.60	7.73	45.51	45.46
444.68	6.94	43.31	43.25
444.69	6.59	41.67	41.62
444.67	6.37	40.41	40.35
444.68	6.19	39.08	39.02
444.72	6.03	37.84	37.78
444.72	5.85	36.35	36.29
444.75	5.64	34.93	34.86
444.77	5.37	32.99	32.92
444.79	5.05	30.86	30.79
443.69	4.72	29.48	
443.87	4.29	27.65	
443.91	3.85	26.46	
443.91	3.30	25.24	25.24
444.02	2.73	24.39	24.39
444.37	2.37	24.33	24.29
444.40	2.18	24.33	24.29
444.40	1.92	24.08	24.04
444.28	1.34	23.48	23.44
444.41	0.87	23.08	23.04
444.42	0.48	22.48	22.44
$T_{\text{nom}} = 504 \text{ K}$			
504.3	18.60	52.45	52.42
504.3	17.21	51.08	51.05
504.4	15.19	48.87	48.83
504.5	12.68	45.63	45.58
504.6	10.11	41.23	41.17
504.2	10.11	41.11	41.09
504.3	8.10	36.86	36.83
504.4	6.06	33.05	33.01
504.4	4.05	30.43	30.39
503.6	2.02	29.79	29.83
503.7	2.02	29.76	29.79
503.7	0.99	28.76	28.79
503.9	0.47	28.28	28.29

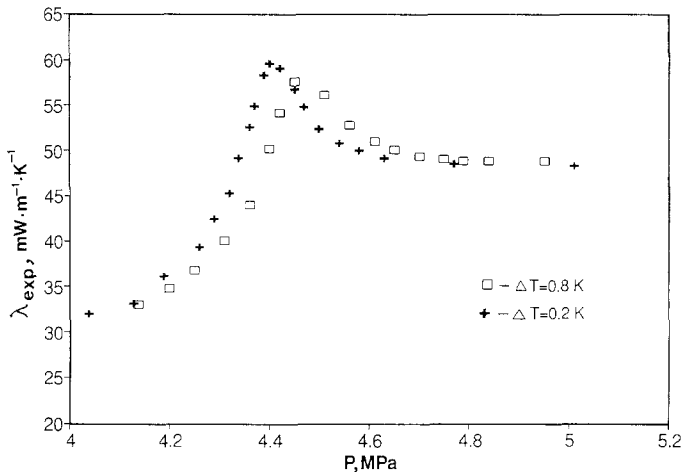


Fig. 2. The thermal conductivity of 1-chloro-1,1-difluoroethane for  $T=415.0$  K and  $T=415.5$  K obtained, respectively, with temperature differences  $\Delta T=0.2$  K and  $\Delta T=0.8$  K.

The application of the steady-state coaxial-cylinder apparatus near the critical point has been the subject of some controversy, caused by the possible presence of heat transfer by convection, simultaneous with the conduction mode. We have made two sets of measurements at the isotherm around 415 K with different temperatures differences  $\Delta T$  between the cylinders. The results obtained are shown in Fig. 2 for  $\Delta T=0.2$  and 0.8 K. It is noteworthy that  $T - T_c \approx 5$  K for both sets of measurements and that there is no variation in the values obtained with the higher  $\Delta T$  from the values for  $\Delta T=0.2$  K that can be attributed to convection. The displacement between the two curves is completely explained by the slightly different average temperatures of the two sets of data (415.0 and 415.5 K). We can therefore conclude that the present data are free from any type of convective effects.

#### 4. DATA ANALYSIS

The data analysis can be separated into three zones, the gaseous state ( $T < T_c$ ), the liquid state, and the supercritical region ( $T > T_c$ ). The lack of experimental density data for the supercritical fluid region excludes any theoretical comparison with existing approaches in this region.

#### 4.1. The Gaseous State

From the experimental data we can derive, at each temperature, dilute gas values ( $P = 0$ ) by graphical extrapolation of the data obtained at lower pressures. The resulting dilute gas values were found to have a quadratic temperature dependence and can be represented by

$$\lambda(0, T) = -5.5597 + 3.9562 \times 10^{-2}T + 5.475 \times 10^{-5}T^2 \quad (7)$$

where  $\lambda$  is in  $\text{mW} \cdot \text{m}^{-1} \cdot \text{K}^{-1}$  and  $T$  is in K. The mean square deviation of the fit is  $\sigma = 0.07 \text{ mW} \cdot \text{m}^{-1} \cdot \text{K}^{-1}$  (0.52% at lower temperatures and 0.25% at higher temperatures). The extrapolated values are presented in Table IV and are shown in Fig. 3, together with the results obtained by other investigators. Also represented are the values from the Vargaftik tables [6]. The present results agree with their mutual uncertainty with the results of the tables, which were constructed mainly on the basis of the results obtained by Tsevetkov [5]. The results of Afsar and Saxena [3] are about 10% higher than the present results at temperatures below 400 K, agreeing within mutual uncertainty at lower temperatures. This is possibly due to radiative heat transfer in the thermal conductivity column used [3]. The results obtained by Fellows et al. [4] were measured with a transient hot-wire instrument, using a single platinum wire, and although their claim of accuracy is 3%, the use of a bare single wire in polar fluid measurements must have degraded the accuracy of the data. This set of data is systematically higher than the present data by about 14%, and no other reason was found for this discrepancy.

Table IV. Zero-Pressure and Saturation-Line Thermal Conductivity of HCFC-142b

$T$ (K)	$\lambda(0, T)$ ( $\text{mW} \cdot \text{m}^{-1} \cdot \text{K}^{-1}$ )	$\rho_{\text{sat}}(T)$ ( $\text{kg} \cdot \text{m}^{-3}$ )	$\lambda(\rho_{\text{sat}}, T)$ ( $\text{mW} \cdot \text{m}^{-1} \cdot \text{K}^{-1}$ )
290		1130	82.8
293		1123	81.7
330	13.50	1024	69.4
368	16.35	890.6	58.0
403	19.20	705.0 <sup>a</sup>	48.8
415	20.34		
426	21.23		
444	22.87		
504	28.26		

<sup>a</sup> Point obtained from Ref. 13.

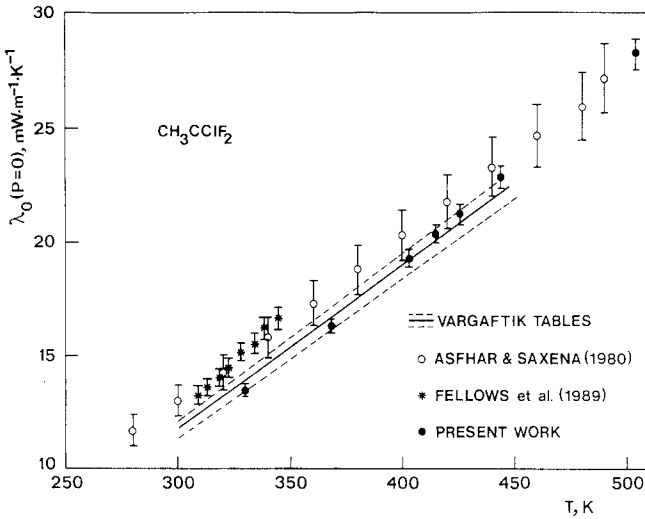


Fig. 3. The zero-pressure value of the thermal conductivity of 1-chloro-1,1-difluoroethane (HCFC-142b) as a function of temperature. (---) Ref. 6; (○) Ref. 3; (\*) Ref. 4; (●) present work.

The value of  $d\lambda(0, T)/dT$  at each nominal temperature was obtained from Eq. (6) by direct derivation.

#### 4.2. The Liquid State

The liquid-state isotherms measured cover a range of states from 290 to 403 K, from the saturation line to 20 MPa. This includes a density range of 700 to 1200  $\text{kg}\cdot\text{m}^{-3}$ .

The values of the excess thermal conductivity,  $\Delta\lambda(\rho, T)$ , defined as

$$\Delta\lambda(\rho, T) = \lambda(\rho, T) - \lambda(0, T) \tag{8}$$

were calculated for the liquid phase, with the density values obtained from Eqs. (5) and (6). Figure 4 shows the excess thermal conductivity of HCFC-142b as a function of density. No temperature dependence was observed. The excess can be translated by the equation

$$\begin{aligned} \Delta\lambda(\rho, T) = & -0.23363 + 9.3271 \times 10^{-2}\rho - 1.4978 \times 10^{-4}\rho^2 \\ & + 1.09726 \times 10^{-7}\rho^3 \end{aligned} \tag{9}$$

with  $\Delta\lambda$  in  $\text{mW}\cdot\text{m}^{-1}\cdot\text{K}^{-1}$  and  $\rho$  in  $\text{kg}\cdot\text{m}^{-3}$  within  $0.27 \text{ mW}\cdot\text{m}^{-1}\cdot\text{K}^{-1}$ . The deviations of the experimental points never exceed  $\pm 1\%$ .

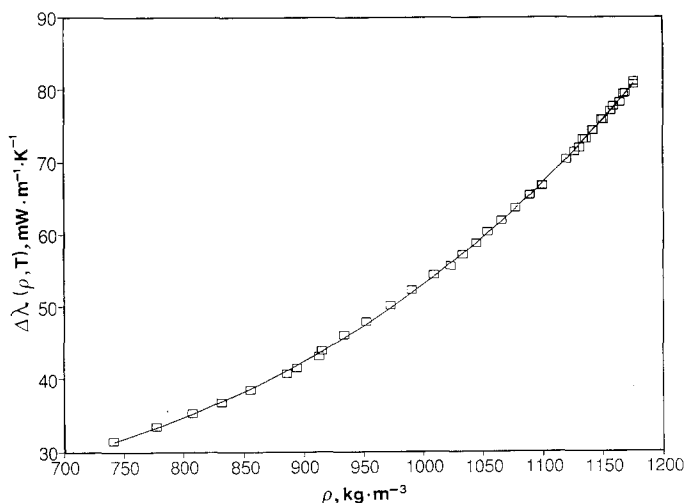


Fig. 4. The excess thermal conductivity of 1-chloro-1,1-difluoroethane (HCFC-142b) as a function of density in the liquid region. (□) Experimental points; (—) Eq. (9).

The data obtained can be compared only with data from the Vargaftik tables [6] at the saturation line. At 293 K the tables quote a value of  $86.9 \text{ mW} \cdot \text{m}^{-1} \cdot \text{K}^{-1}$ , while our value is  $81.35 \text{ mW} \cdot \text{m}^{-1} \cdot \text{K}^{-1}$  at the lowest pressure. The difference between these two values is  $-6.8\%$ , which is larger than the claimed uncertainty of the tables ( $3\%$ ) and of our data ( $2\%$ ). At 333 K the difference decreases to about  $-4.4\%$ . The isotherm at 368 K is already outside the table values. Extrapolation of those values indicates, however, that an agreement of  $-2.5\%$  is obtained, which is already commensurate with the mutual uncertainty of the data presented and that of the tables [6].

The values of the thermal conductivity of HCFC-142b were extrapolated to the saturation boundary using the equation for liquid region herein presented and the values of the excess function taken from Eq. (9) and the dilute gas values taken from Eq. (7). The values obtained are presented in Table IV. The thermal conductivity of 1-chloro-1,1-difluoroethane along the saturation line varies linearly with temperature, as expected, and can be represented by the equation

$$\lambda_{\text{sat}}(T) = 170.39 - 0.3036T \quad (10)$$

to within  $0.80 \text{ mW} \cdot \text{m}^{-1} \cdot \text{K}^{-1}$ .

A comparison with the thermal conductivity of CFC-114, dichlorotetrafluoroethane, in the saturation line [19], shows that HCFC-142b has

a thermal conductivity 30% greater than that of CFC-114 at the same reduced temperature and, therefore, a higher efficiency as a heat transfer fluid.

### 4.3. The Supercritical Region

We have made an extensive experimental study of the thermal conductivity of 1-chloro-1,1-difluoroethane in the supercritical region, at four different temperatures (pseudo-isotherms near the critical point). Unfortunately, it was not possible to make measurements at temperatures above

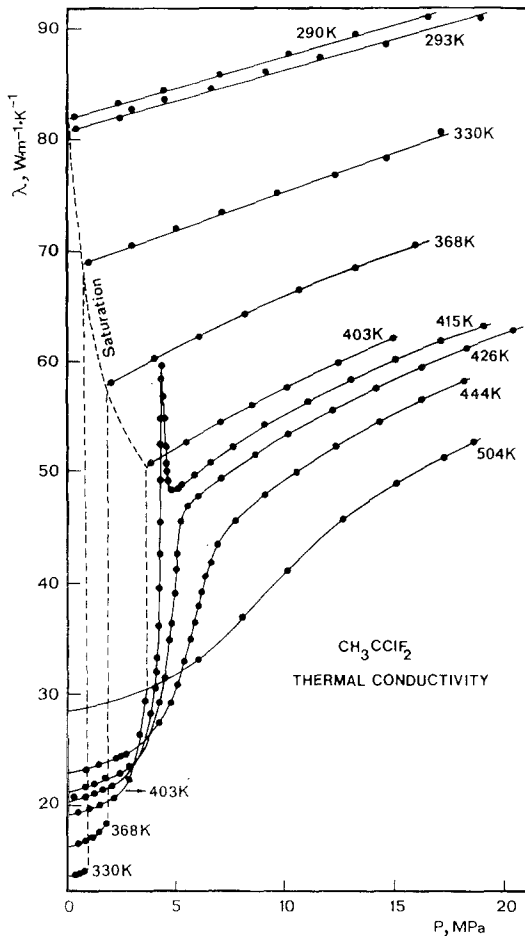


Fig. 5. The thermal conductivity of 1-chloro-1,1-difluoroethane (HCFC-142b) as a function of pressure and temperature.

504 K ( $T/T_c = 1.23$ ) and the higher-temperature isotherm still exhibits a strong critical enhancement. Therefore, it was not possible to select a background thermal conductivity function because of this problem and because of the lack of density data for this region. The data analysis cannot proceed in a fashion similar to the other systems already studied by the authors, as in the case of *n*-butane [10].

Figure 5 displays the complete data set obtained, including the liquid and gas zone, as a function of pressure, for all the investigated isotherms. The critical enhancement in the  $(\lambda, P)$  diagram is very large, but it can be well defined only when density data for this zone become available.

## 5. CONCLUSIONS

The thermal conductivity of 1-chloro-1,1-difluoroethane (HCFC-142b) has been measured for a wide range of thermodynamic states with an estimated overall accuracy of 2% with a steady-state concentric-cylinder apparatus. The liquid state, the gaseous state, and the supercritical fluid states have been covered. The present data represent the most extensive study of this property for HCFC-142b.

Although the authors have measured the density of HCFC-142b in the liquid region and in some part of the gaseous region, there are no data available for the supercritical region and therefore a complete study of the critical enhancement cannot be performed at present.

## ACKNOWLEDGMENTS

This work was partially funded by INIC/JNICT/CNRS protocol. The authors are indebted to ATOCHEM, France, for having supplied the HCFC-142b sample.

## REFERENCES

1. M. O. McLinden and D. A. Didion, *ASHRAE J.* **21**:32 (1987).
2. M. O. McLinden and D. A. Didion, *Int. J. Thermophys.* **10**:563 (1989).
3. R. Afsar and S. C. Saxena, *Int. J. Thermophys.* **1**:51 (1980).
4. B. R. Fellows, R. G. Richard, and I. R. Shankland, in *Thermal Conductivity 21*, C. T. Creemers and A. Fine, eds. (Plenum Press, New York, 1990).
5. O. B. Tsvetkov, *Inzh. Fiz. Zh.* **9**:810 (1969).
6. N. B. Vargaftik, *Tables on the Thermophysical Properties of Liquids and Gases*, 2nd ed. (Hemisphere, Washington, DC, 1975).
7. B. Le Neindre, Thesis (Université Paris VI, Paris, 1969).
8. R. Tufeu, Thesis (Université Paris VI, Paris, 1971).
9. R. Tufeu and B. Le Neindre, *High Temp. High Press.* **13**:31 (1981).
10. C. A. Nieto de Castro, R. Tufeu, and B. Le Neindre, *Int. J. Thermophys.* **4**:11 (1983).



11. C. A. Nieto de Castro, in *Supercritical Fluid Technology*, J. Ely and T. Bruno, eds. (Chemical Rubber Co., Boca Raton, FL, 1991).
12. A. T. Sousa, C. A. Nieto de Castro, R. Tufeu, and B. Le Neindre, *High Temp. High Press.* 1991 (in press).
13. Y. Maezawa, H. Sato, and K. Watanabe, *Proc. 10th Symp. Thermophys. Prop.* (JSME, Tokyo, 1989).
14. R. DeSantis, F. Gironi, and L. Marreli, *Ind. Eng. Chem. Fundam.* **15**:183 (1976).
15. F. H. Ree and W. G. Hoover, *J. Chem. Phys.* **40**:939 (1964).
16. J. Erpenbeck and W. W. Wood, *J. Stat. Phys.* **35**:32 (1984).
17. A. T. Sousa, P. J. S. Fialho, C. A. Nieto de Castro, R. Tufeu, and B. Le Neindre, submitted for publication (1991).
18. M. O. McLinden, *Proc. ASHRAE CFC Technol. Conf.*, Gaithersburg, MD, Sept. (1989).
19. J. Yate, T. Minamiyama, and S. Tanaka, *Int. J. Thermophys.* **5**:209 (1984).